DOI: 10.1002/asia.200600125

Dendrimeric Bisphosphonates for Multivalent Protein Surface Binding

Markus Arendt, Wei Sun, Jens Thomann, Xiulan Xie, and Thomas Schrader*[a]

Abstract: A single weak-binding event is multiplied into an efficient receptor site for protein surfaces ($<10^{-1}$ to $>10^{6}\,\text{M}^{-1}$ in buffered aqueous solution) in a biomimetic fashion. This has hitherto been done with natural host/guest pairs, but not with artificial receptors. The organic reaction presented is one of very few that enable chemists to fuse multiple ionic building blocks covalently in highly polar solution; this one-pot reaction proceeds with virtually quantitative yield. According to this concept, other building blocks with aldehyde groups can likewise be multiplied into monodisperse functional dendrimers. Small basic proteins are bound by octameric dendrimers in 1:1 or 1:2 complexes with millimolar to submicromolar affinities. The complexation event is studied independently in buffered aqueous solution by three different spectroscopic methods (PFG-LED, UV/Vis, and fluorescence). Potential new applications include recombinant protein purification through Arg tags on immobilized dendrimers and on/off switching of protein function by reversible active-site capping of enzymes.

Keywords: dendrimers · multivalency · proteins · reduction amination · surface recognition

Introduction

For efficient and selective molecular recognition processes on surfaces, nature often applies the concept of multivalency:[1] single weak-binding events are multiplied either because the approaching guest, usually a protein, carries many identical binding sites or because the surface offers an array of multiple similar receptor sites. Binding energies usually increase enormously as a consequence of the favorable entropy balance for the subsequent binding events, which take advantage of preorganization.[2] Cell surface recognition provides many instructive examples for this principle: the influenza virus attaches to its target cell by way of multiple simultaneous interactions between hemagglutinin (HA) trimers on its own surface and sialic acids (SA) densely packed on the cell surface;[3] fibronectin, a soluble glycoprotein with a large number of arginine–glycine–aspartate (RGD) tripeptide fragments on solvent-exposed loops, docks onto membrane-bound integrins presented by epithelial cells.[4] Similarly, neutrophils attach to endothelial cells close to the site of injury through polyvalent interactions,[5] antibodies recognize their antigens with multiple receptor sites,[6] and oligomeric transcription factors bind to multiple sites on DNA.[7] In summary, the concept of multivalency finds widespread use in biology and often collectively results in dramatically enhanced interaction.

Supramolecular chemists have started to imitate this powerful concept and develop artificial receptor molecules with multiple binding sites. Whitesides and co-workers dimerized and later also trimerized the efficient antibiotic vancomycin and achieved extremely strong binding to the Lys-D-Ala-D-Ala sequence found ubiquitiously in bacterial cell walls.[8] Bundle and co-workers invented a pentameric carbohydrate inhibitor called "starfish", which was specific for and exceedingly active against shiga toxin.[9] Similarly, a high-affinity inhibitor for cholera toxin required a fivefold attachment of an α-D-galactoside (MNPG) to a pentacyclen core unit.[10] Postsynthetically modified (PSM) polymers in the form of multivalent mannose displays nonspecifically inhibit hemagglutination.[11] Specific recognition of phosphorylated peptides and proteins was realized by a fluorescent chemosensor carrying two Zn^{II}–dipicolylamine units.[12] Multivalent transition-metal complexes were designed to match the histidine surface pattern of carbonic anhydrase.[13] Anionically functionalized amphiphilic nanoparticles (i.e., monolayer-protected gold clusters; MMPCs), on the other hand, use

[a] Dr. M. Arendt, W. Sun, J. Thomann, Dr. X. Xie, Prof. Dr. T. Schrader
Fachbereich Chemie der Universität
Hans-Meerwein-Straße
35032 Marburg (Germany)
Fax: (+49) 642-128-28917
E-mail: schradet@staff.uni-marburg.de

Supporting information for this article is available on the WWW under http://www.chemasianj.org or from the author.

nonspecific interactions to inhibit chymotrypsin efficiently through electrostatic binding followed by protein denaturation.[14] Finally, aspartate-rich cyclopeptides on calixarene scaffolds or glutamate-rich peptides on porphyrins were recently developed for cationic protein surface recognition.[15] In the challenging area of protein epitope mimetics, considerable progress was recently achieved with β-hairpin scaffolds.[16] These can even be combinatorially generated for automated biological screening. Similarly, functionalized helix–loop–helix motifs have been used in an elegant way to control recognition and catalyst properties of designed protein receptors.[17]

In recent years we introduced *m*-xylylene bisphosphonates **1** as receptor units for lysine and arginine residues in a peptidic environment.[18] However, as the binding event relied mostly on electrostatic interactions, even in organic solvents their affinity dropped drastically with increasing solvent polarity (DMSO: $\approx 25000\,\text{M}^{-1} \rightarrow$methanol: $800\,\text{M}^{-1}$). In water, almost no attraction of basic peptides occurred. The question of whether multiplication of the single weak interactions would recover the efficient recognition of basic peptides in water and at the same time impose specificity for accumulated basic amino acids over isolated arginines or lysines (Figure 1) therefore arose.

The new dimer and trimer showed no appreciable self-association, as judged from dilution experiments, but distinct chemical-shift changes were observed during NMR spectroscopic titrations in methanol with RR (diarginine) and RRR (triarginine).[19] Nonlinear regression analysis of the resulting binding isotherms produced binding constants that were much higher than those of single host–guest interactions: a 2:1 complex (Job plot) with $K_a = 42\,000\,\text{M}^{-1}$ for each individual complexation step was found for the dimer with H-Arg-Arg-OH, and a somewhat less pronounced increase in K_a to $60\,000\,\text{M}^{-1}$ for the trimer with H-Arg-Arg-Arg-OH, this time in the much more efficient 1:1 stoichiometry. Considering the substantial structural difference in the spacer units of dimer **2** and trimer **3**, the 50- and 75-fold increases in K_a agree very well with the multiplication of binding events postulated above due to the covalently interconnected receptor units. Even more promising is the relatively high association constant for the trimer/RRR interaction in 50% aqueous methanol, which still amounts to $16\,000\,\text{M}^{-1}$, probably due to additional hydrophobic interactions between both host and guest backbones (dotted lines in Figure 1b.). However, for a binding mechanism that relies mainly on Coulomb interactions, even a 1:1 methanol/water mixture (necessary for complete dissolution of **2** and **3**) is far less competitive than a buffered aqueous or even physiological solution.

Results and Discussion

Dendrimer Synthesis

The conventional synthesis of higher oligomers proved problematic, because even with dialkylphosphonate protecting groups, the products are water-soluble and cannot undergo chromatography over silica gel or reverse phases (RPs). Furthermore, a stepwise and therefore nonconvergent construc-

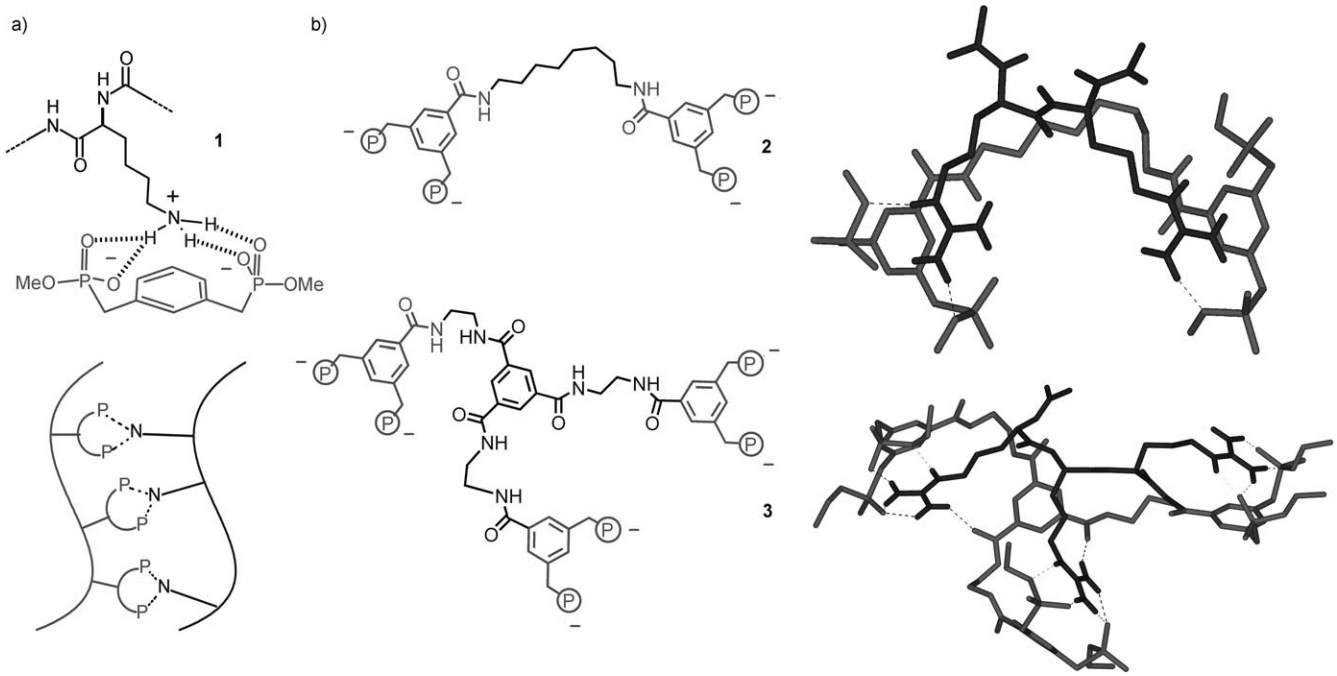

Figure 1. a) Top: Monomeric bisphosphonate **1** binding to the lysine side chain in its peptidic environment. Bottom: Schematic illustration of the multiplication of this binding event by covalent oligomerization. b) Lewis structures of dimeric and trimeric bisphosphonate **2** and **3** depicted on the left in the same conformation as in their corresponding 1:1 complexes with di- and triarginine on the right, calculated with MacroModel 7.0 (Amber*, water, Monte Carlo simulation, 2000 steps). Ⓟ = methylphosphonate monolithium salt.

tion of large molecules suffers from a clear disadvantage in synthesis economy. These difficulties can be circumvented by starting from dendrimer cores and simultaneously attaching binding sites to their periphery.[20] Polypropyleneimine (PPI) dendrimers are commercially available in various generations and offer a similar number of bridging atoms between their amine end groups as **2** and **3**. Moreover, initial modeling experiments suggest that in spite of their dendritic nature, almost every binding site can find its arginine counterpart on a flat surface, such as that of a protein.[21] An ideal solution would directly furnish the free phosphonate salts in quantitative yield. However, to date, few organic reactions are known that involve multiply charged ionic species in highly polar solution. Kiessling and co-workers developed the Staudinger reaction for native chemical peptide ligation,[22] von Kiedrowski and co-workers used acylhydrazone formation for the construction of DNA hybrids,[23] and Sharpless and co-workers obtained covalent modifications of biomolecules in living systems with "click chemistry".[24] With the PPI dendrimer polyamines at hand, we examined a multiple reductive-amination sequence (Figure 2).[25]

To this end, a bisphosphonate benzaldehyde derivative was prepared and bisdealkylated with LiBr to the corresponding dilithium salt.[26] This building block was dissolved in methanol and reacted in a 1:1 ratio with each amine end group of the dendrimer. Subsequent $NaBH_4$ addition in the same pot converted the unstable Schiff base into the stable benzylamine (Figure 3a).[27] Its ^1H and ^{31}P NMR spectra displayed a clean set of slightly broadened signals, confirming quantitative conversion of the imine intermediate into the desired reduced state (Figure 3b).[28]

To remove excess borate salts, the respective bisphosphonate tetramer **4**, octamer **5**, and hexadecamer **6** were also purified by RP-HPLC and characterized by MALDI-TOF MS. The three dendrimeric host generations obtained were not monodisperse, but consisted of oligomer families with a high degree of phosphorylation (e.g., the octamer contained 5–8 mers).[29] They were all very soluble in water.

Dendrimer Characterization

An important question remained to be answered with reference to the receptor structure in buffered aqueous solution: Will the charged amine core of the zwitterionic dendrimers attract the bisphosphonate binding sites and eventually lead to an inner collapse, also known as backfolding?[30] Extended Monte Carlo simulations with MacroModel suggested an open structure without significant intramolecular salt bridges;[31] dilution experiments did not indicate any self-association processes. If this is correct, the spherical diameter of each dendrimer generation must reflect the calculated monomer size, irrespective of the surrounding pH.[32] Zwitterionic dendrimers are known to adopt an extended conformation with a maximal hydrodynamic volume, both at very low and very high pH values. The reason is electrostatic repulsion of all positive charges, in our case in the inner amine core, or all negative ones in the phosphonate periphery. At neutral pH, however, a potential inner collapse will lead to a densely packed species with a markedly reduced volume. It should be emphasized, however, that PPI dendrimers similar to all dendrimers containing aliphatic tertiary amines have markedly a decreased R_3N p*K*a value of 5.9; at neutral pH, half of them are protonated, whereas the secondary peripheral ammonium groups are still strongly basic and hence fully protonated (p*K*a $\approx$ 9).[33] This amounts to a total charge of −3, −5, and −9 for **4**, **5**, and **6**, respectively. We determined the hydrodynamic volume of **3** at three different protonation states with NMR diffusion measurements (Figure 4).[34] In a typical PFG-LED (pulsed field gradient longitudinal eddy current delay) experiment, a value of 14.5 Å was determined for the dendrimer radius in neutral medium (Table 1), in good agreement with the calculated value (14.9 Å). Transition to pH 2 or pH 10 only led to minute changes ($d = 14.3$ and 14.7 Å), indicating that indeed no backfolding occurs in the zwitterionic dendrimer. As an important consequence, all bisphosphonate moieties are available for protein recognition. This result was independently reached by Monte Carlo simulations of the octa-

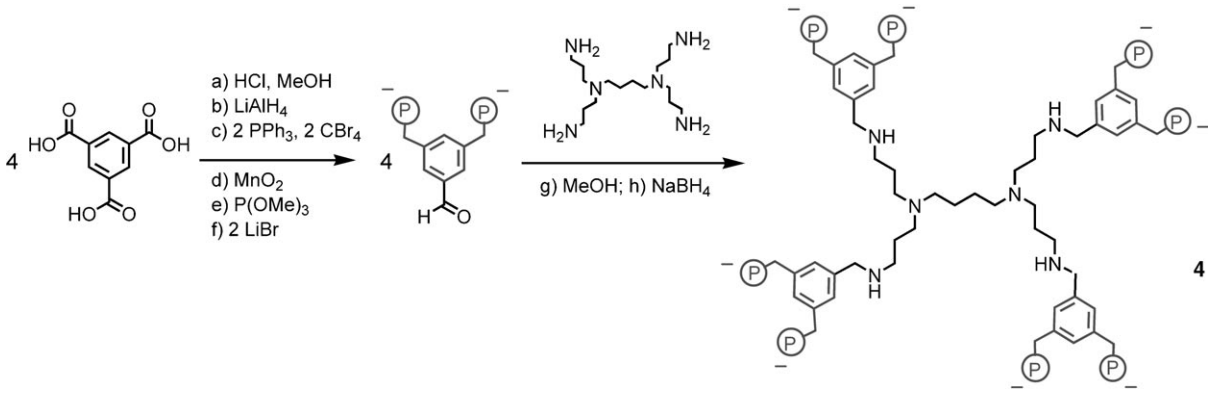

Figure 2. Synthesis of the ionic bisphosphonate building block and subsequent one-pot reaction with the first-generation PPI core by a multiple reductive amination sequence. Yields: a) 98%; b) 81%; c) 60%; d) 95%; e) 95%; f) 92%; g) 99%; h) 98%. The octamer and hexadecamer were prepared by the same route in comparable yield.

CHEMISTRY
AN ASIAN JOURNAL

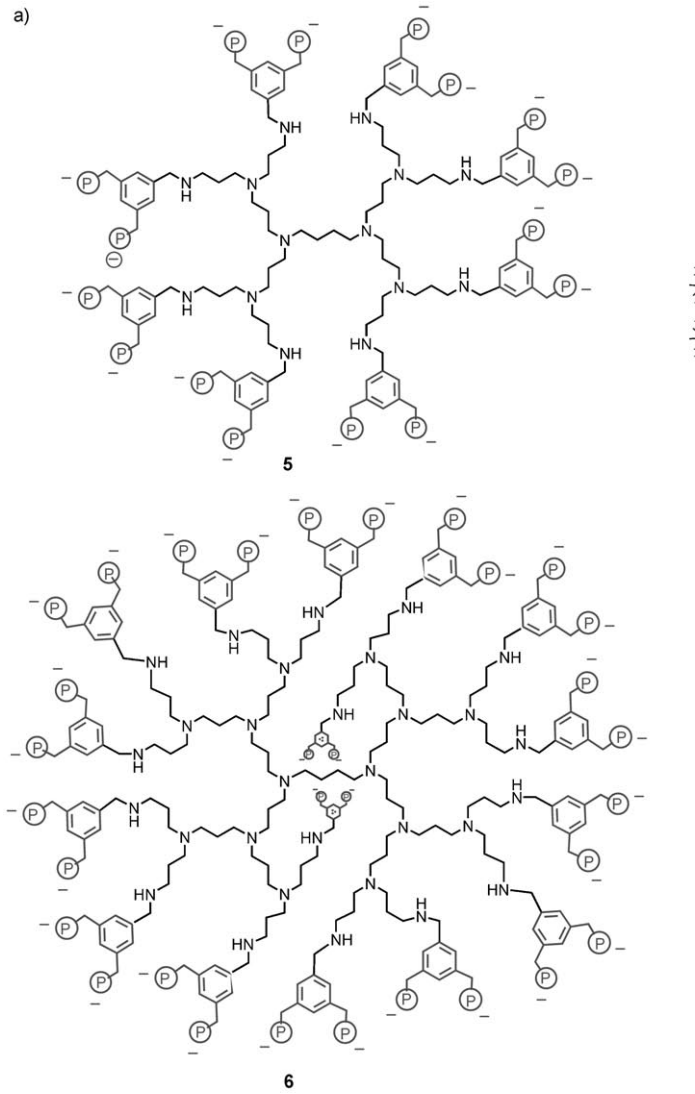

Figure 3. a) Lewis structures of **5** (octamer) and **6** (hexadecamer). b) ^{31}P and ^{1}H NMR spectra of the crude octameric bisphosphonate (400 MHz, D_2O).

mer at the three corresponding protonation states (Figure 4).

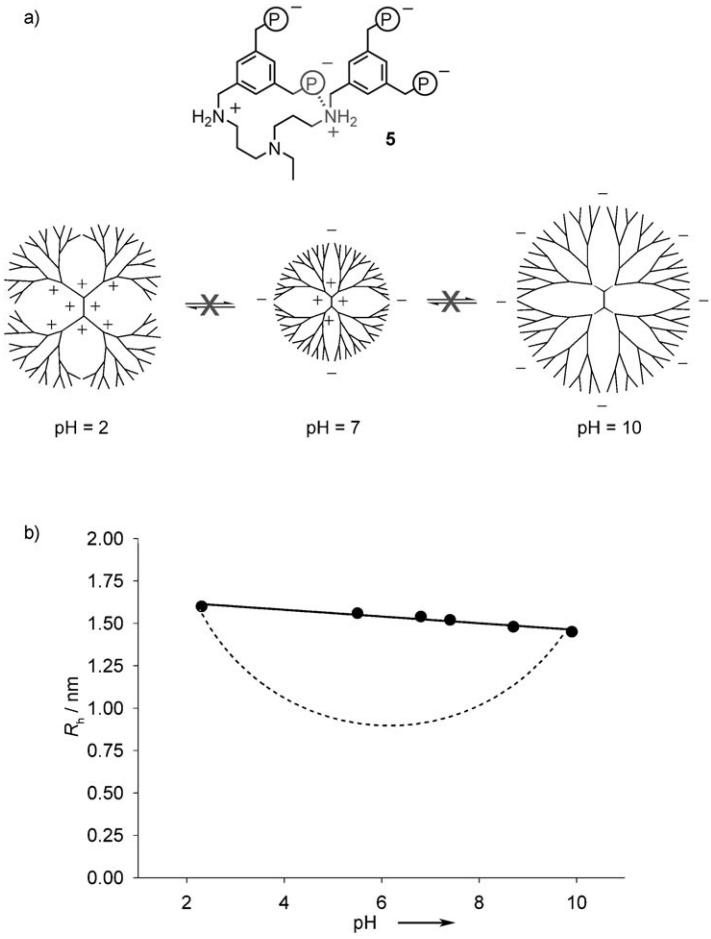

Figure 4. a) Potential inner collapse of zwitterionic dendrimers such as **5** at neutral pH due to electrostatic attraction between phosphonate anions and secondary ammonium groups. b) However, the dendrimer radii, determined by PFG-LED, are almost pH-independent. Confirmation comes from Monte Carlo simulations with the fully protonated, the zwitterionic (shown in a)), and the fully deprotonated octamer.

Table 1. Diffusion coefficient D_0 and measured as well as calculated hydrodynamic radius R_h of octamer **5** at different pH values.

pH	D_0 [10^{-10} $m^2 s^{-1}$]	R_h [Å][a]	$R_{h\,calcd}$ [Å][b]
2.3	1.69	14.5	(1): ≈14.4
5.5	1.66	14.8	≈14.4
6.8	1.62	15.3	(2): ≈13.7
7.4	1.60	15.4	≈13.7
8.7	1.57	15.6	(3): ≈14.1
9.9	1.54	16.0	≈14.1

[a] Hydrodynamic radius. [b] Calculated by molecular modeling. Three structures were modeled: fully protonated (1), deprotonated phosphonates and protonated amines (2), and fully deprotonated (3).

Binding Studies

Diffusion Measurements

As tight complex formation between a small ligand and a large target molecule drastically lowers the diffusion velocity of the ligand, PFG-LED measurements can also be used to determine association constants (Table 2).[35] However,

Table 2. Diffusion coefficients (D) and dissociation (K_d) and association (K_a) constants for complex formation between tetramer **4** and various proteins.

Sample	D [10^{-10} m^{2}s^{-1}]	$K_{d\,calcd}$ [10^{-4} M]	K_a [M^{-1}]
free Cyt *c*	1.662		
free BP tetramer	2.895		
complex Cyt *c*/tetramer	2.759	2.92	3424[a]
free chymotrypsin	1.482		
complex chymotrypsin/tetramer	2.565	6.42	1560[b]
free BSA	0.633		
complex BSA/tetramer	2.591	2.24	2360[c]

[a] 2:1 stoichiometry according to UV/Vis measurements. [b] Unknown stoichiometry, therefore assumed as 1:1. [c] 3:1 stoichiometry according to the fluorescence measurements. BP = bisphosphonate dilithium salt.

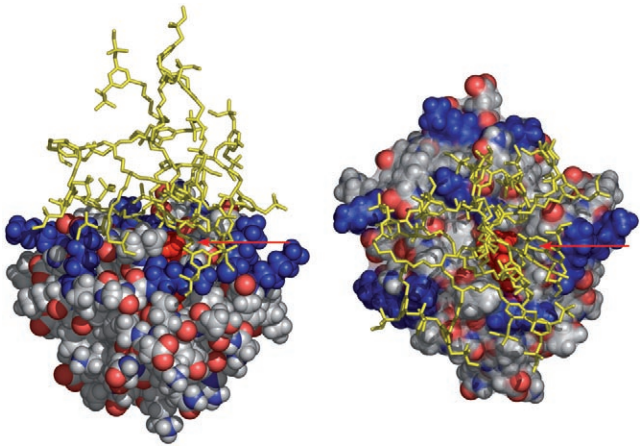

Figure 5. Minimized 1:1 complex between cytochrome *c* (C: grey, O: red, N: blue, lysines around the active site: blue) and the hexadecamer dendrimer (yellow; SYBYL 6.9, MMFF94). Left: side view. Right: top view (protein with transparent Connolly surface and buried heme group in red, arrow).

only the tetramer is small enough to produce a significant difference in diffusion coefficient D compared to a basic protein such as cytochrome *c* (Cyt *c*) (**2**: $D = 2.895 \times 10^{-10}$ m^{2}s^{-1}; free Cyt *c*: $D = 1.662 \times 10^{-10}$ m^{2}s^{-1}). Its K_D values with various proteins in neutral phosphate buffer are typically in the millimolar range. Thus, the induced deceleration of **4** on complex formation between both analytes was calculated to be equivalent to a K_a value of about 3400 M^{-1} (10 mM NaH_2PO_4, 1 mM Cyt *c*, pI 9.5, 12 kD; Table 3). Less-

Table 3. Binding affinities and complex stoichiometries for various proteins and the tetrameric bisphosphonate dendrimer according to PFG-LED measurements in aqueous buffer (1 mM protein in 10 mM NaH_2PO_4).

Protein	pI	Stoichiometry	K_a (each step) [M^{-1}]
cytochrome *c*	9.5	2:1	3400
chymotrypsin	8.0	1:1	1600
BSA	6.0	3:1	2400

basic chymotrypsin (pI 8.0) gives a K_a value of 1600 M^{-1}. Bovine serum albumin (BSA) contains many more-acidic amino acids (pI 6.0), but also is much larger in size (82 kD) and carries several basic domains on its surface, so that in principle several dendrimers can bind at the same time. In this case, PFG-LED estimates a binding constant of 2400 M^{-1}, assuming a 3:1 stoichiometry.[36]

UV/Vis Titrations

Unfortunately, the same experiments cannot be carried out with the higher oligomers, because their hydrodynamic volume approaches that of the proteins and leads to large intrinsic errors. However, Cyt *c* carries its porphyrin molecule buried directly beneath the protein surface and surrounded by eight lysines (Figure 5). A tight ionic dendrimer cap can be predicted to influence the absorption behavior of this chromophore, thus rendering the whole protein molecule sensitive to a UV/Vis titration experiment.[37] This was indeed the case, although small absolute changes and large data scattering qualifies the obtained data as mere estimates of K_a. For clarity and a better comparison, association constants were initially calculated for each single binding step, assuming no cooperativity. Thus, a 1:2 complex between protein and dendrimer was always calculated as if two 1:1 binding events were happening consecutively, with identical affinities for both equilibria. In spite of their approximate character, the respective K_a values clearly reveal a steadily rising binding affinity towards Cyt *c* from the tetramer (5×10^3 M^{-1}; 2:1) to the octamer (1×10^4 M^{-1}; 2:1) and hexadecamer (6×10^4 M^{-1}; 1:1), thus confirming the validity of the multivalency concept.

Fluorescence Titrations on Labeled Proteins

To extend the scope of our new protein binders to any desired protein, we had to overcome the limitation of a natural built-in chromophore. To this end, we incorporated a fluorescent label (OregonGreen[38] or fluorescein) in several interesting proteins of varying pI and surface structure. OregonGreen is known to address selectively the N terminus of a given protein at pH 8.4 with minimal change in protein tertiary structure and virtually no concomitant loss in activity. We introduced this label into proteins with pI values between 6 and 10.5 and purified the singly labeled targets by gel permeation chromatography (GPC). The resulting strongly fluorescent protein derivatives were incubated with increasing amounts of the dendrimer binders and examined at the intensity maximum of their fluorescence emission (Figure 6). In several cases, the fluorescence intensity rose significantly and produced a saturation curve, from which protein affinities could be derived. Approximate K_a values were thus determined from fluorescence titrations at 10^{-5} M concentrations in NaH_2PO_4 buffer (10^{-2} M) (data not shown). In general, transition from a dendrimer generation to the one higher leads to a significant increase in K_a of roughly one order of magnitude, now reaching 4×10^5 M^{-1} for the most efficient pair, **5**/chymotrypsin. Unfortunately, the

CHEMISTRY
AN ASIAN JOURNAL

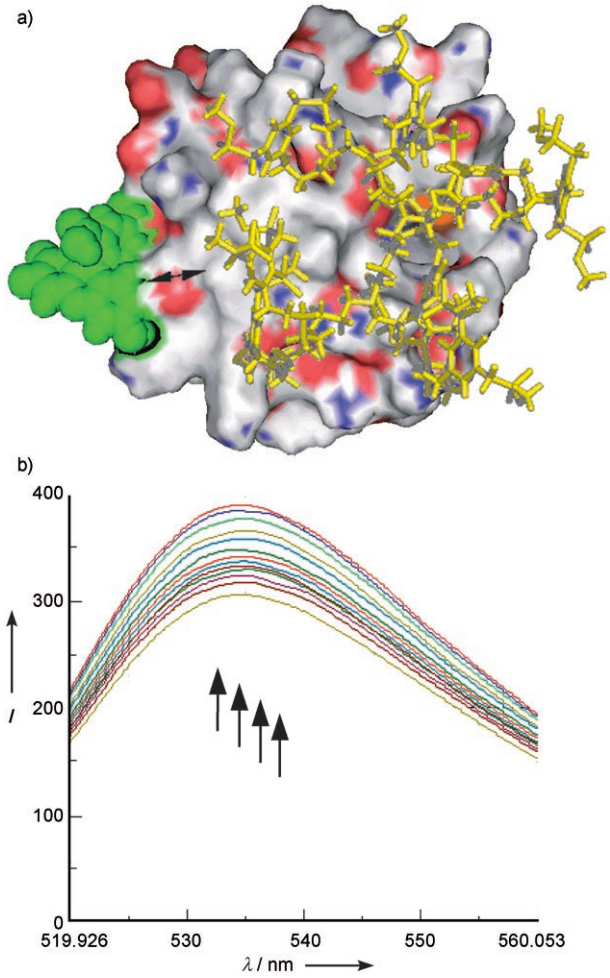

Figure 6. a) Diagram detailing the principle of the fluorescence assay: an octamer dendrimer (yellow) caps the active site of Cyt *c*, leading to interference with the fluorescence label (green) located in its vicinity. b) Fluorescence curves obtained during a titration of OregonGreen-labeled BSA with the octameric bisphosphonate.

changes in fluorescence intensity were in most cases very small, thus precluding an exact quantitative evaluation. A possible explanation is the location of the N terminus in these proteins: if the fluorescence label is attached far from the basic domain, the dendrimer will also bind remotely from the label and fail to give a fluorescence signal.

Fluorescence Titrations on Labeled Denrimers

The changes in fluorescence emission intensity became much more impressive when the dendrimer itself was tagged with a single fluorescein label (**5a**; Figures 7 and 8). For most proteins with pI values above 7, binding isotherms could be fitted to a 1:1 or 1:2 binding model; the corresponding K_a values, which were again calculated for each individual binding step, roughly follow the pI scale, spanning almost three orders of magnitude. Dissociation constants dropped in some cases to the micromolar regime, especially with small lysine-rich proteins carrying surface-exposed aro-

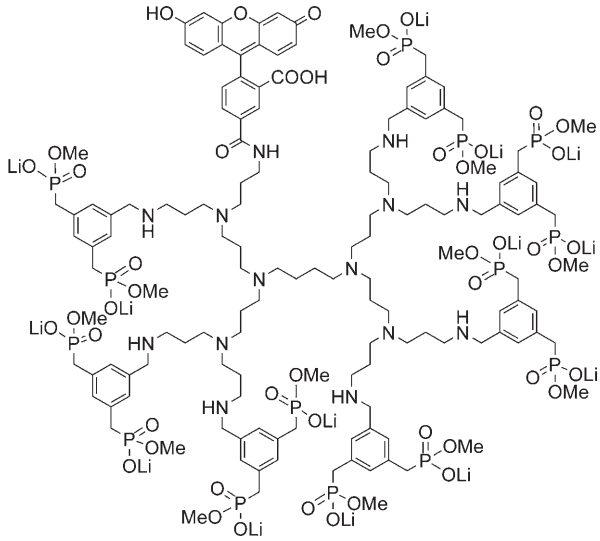

Figure 7. Structure of the fluorescein-labeled octametric bisphosphonate **5a**.

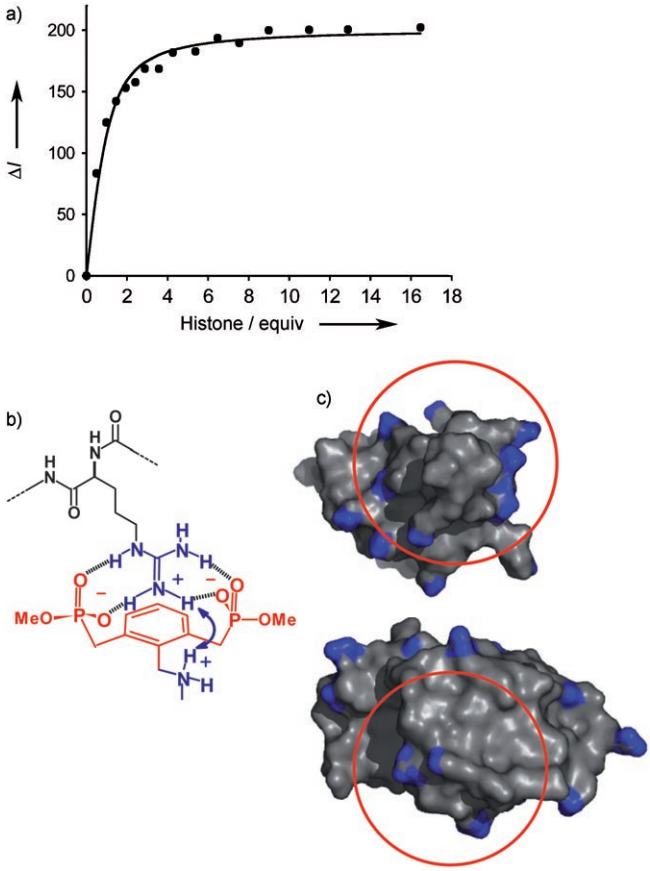

Figure 8. a) Typical fluorescence titration curve obtained from complex formation between fluorescein-labeled **5a** with histone H1. b) Diagram showing the repulsive guanidinium/ammonium interaction preventing formation of the π-cation-stabilized arginine–bisphosphonate complex within the dendrimer. c) Highest density of basic residues on a Connolly surface for histone and lysozyme. The estimated contact area of the hexadecamer dendrimer is depicted in red. Note that histone is lysine-rich, whereas in lysozyme, arginines prevail.

matic residues (histone H1, trypsin; Table 4). Arginine-rich lysozyme, proteinase K, as well as arginine-rich histone H3 produced surprisingly low K_a values, in sharp contrast to the marked arginine selectivity in related polymeric protein hosts. A possible explanation for this unprecedented potential lysine selectivity involves unfavorable Coulomb repulsion between the approaching guanidinium cation of arginine and the unique secondary benzylammonium group, which is present only in the dendrimers owing to the reductive amination step (Figure 8b).[39] Importantly, the stoichiometries determined by means of Job plots for the octamer and hexadecamer and basic proteins were all 1:1 or 1:2, with the exception of large hemoglobin accomodating two dendrimer molecules. The stoichiometries depend mainly on the size of the protein surface and the density of the basic amino acid residues. Thus, it seems highly probable that the dendrimers search for domains of high positive surface charge to exploit multivalent electrostatic attaction. In three cases (histone H3, proteinase K, BSA), one dendrimer could hold two protein molecules; this is surprising, especially in view of the considerable protein size of BSA, but may be connected with local basic domains of high surface charge. Separate calculation of both association constants[40] reveals a distinct preference for the first binding event (negative cooperativity), most likely due to mutual electrostatic repulsion between both protein guests in the second binding step. The results are summarized in Table 5.

Table 4. Association constants and stoichiometries for complex formation between fluorescein-labeled dendrimers **5a**, **6a**, and native proteins of varying pI and size, according to fluorescence titrations in buffered aqueous solution at 25 °C (10 μM protein in 10 mM Hepes buffer).

Protein	Proteins and peptides pI	MW [K]	Arom [%][a]	Lys/Arg[a]	Octamer **5a** K_a [M^{-1}][b]	Ratio	Hexadecamer **6a** K_a [M^{-1}][b]	Ratio[c]
histone H1	10.4	22	3.3	17:12	1×10^6	1:1	–	
histone H3	11.5	15	3.3	13:18	1×10^5	1:2	2×10^4	1:2
Cyt *c*	9.2	12	2.5	16:2	2×10^4	1:1	no effect	–
lysozyme	9.1	14	5.5	7:11	8×10^3	1:1	no effect	–
hemoglobin	8.8	31	5.8	48:9	7×10^3	2:1	–	–
trypsin	8.3	22	5.7	14:2	1×10^6	1:1	2×10^6	1:1
chymotrypsin	8.2	25	3.9	6:8	no effect	–	5×10^5	1:1
proteinase K	7.7	29	8.7	7:9	7×10^4	1:2	–	–
BSA	5.8	66	4.0	41:22	–	–	3×10^4	1:2
ovalbumin	5.3	44	2.0	66:38	no effect	–	–	–
carbohydrate anhydrase	4.5	50	4.4	37:14	no effect	–	–	–
Lys_4	9.5	0.9	0	4:0	6×10^4	1:1	2×10^5	1:1
Arg_4	12.0	1.2	0	0:4	6×10^5	1:1	1×10^5	1:1

[a] The percentage of aromatic contact area and the numbers of lysine and arginine residues on the protein surface were calculated with the atomic volume analysis option in the software PROVE. [b] Triple K_a determinations in selected cases produced experimental errors below 30%. [c] Dendrimer/protein ratio.

Table 5. Binding constants calculated separately for three proteins involved in 1:2 complexes.

Protein	Dendrimer	K^1 [M^{-1}]	K^2 [M^{-1}]
Histone H3	**3a**	1.4×10^5	4.2×10^3
Histone H3	**4a**	4.8×10^5	1.5×10^3
Proteinase K	**3a**	1.8×10^5	1.2×10^3
BSA	**4a**	6.9×10^4	5.1×10^3

Transition from the octamer **5a** to the much larger hexadecamer **6a** does not lead to a drastic increase in affinity. In some cases, K_a values were even smaller (histone H3, Arg_4; Table 4), or no effect was observed on protein addition to the hexadecamer (Cyt *c*, lysozyme; Table 4). Assuming a globular dendrimer topology for both **5a** and **6a**, the hexadecamer is clearly more rigid, thus rendering its induced fit onto a flat protein surface more problematic and limiting its total contact area (Figure 8c).

Another factor that contributes to enhanced protein affinity seems to be the additional hydrophobic interaction between the extended π face of the fluorescein label and aromatic residues on the protein surface (trypsin: $10^4\,M^{-1}$ unlabeled dendrimer vs. $3\times10^5\,M^{-1}$ labeled dendrimer). The appropriate choice of buffer can add to this; for instance, a change from phosphate to Hepes buffer increased the K_a values by another order of magnitude (trypsin: $3\times10^5\,M^{-1}$ phosphate buffer vs. $10^6\,M^{-1}$ Hepes buffer). Remarkably, even physiological salt loads (150 mM NaCl) do not decrease protein affinities (trypsin: $2\times10^6\,M^{-1}$). Finally, a close inspection of EPS (electrostatic potential surface) patterns now offers a plausible explanation for the sensitive discrimination ability between proteins of similar pI and size. Only a fraction of the surfaces of both the dendrimer and the protein (roughly globular) is available for close intermolecular contact. For efficient binding, it is therefore mandatory to ensure a high local density of basic amino acids within this critical cross-section. This is especially true for the relatively small octamer; its contact area is about 8 Å wide. Consequently, arginine residues on the surface of lysozymes, which are on average 12 Å apart from each other, cannot be simultaneously covered by the same ligand. By contrast, histone is densely packed with lysines, and trypsin has a pronounced basic domain at its N terminal, which is ideally suited for multivalent dendrimer docking. We believe that a favorable combination of the factors detailed above inevitably leads to efficient and selective protein surface recognition by bisphosphonate dendrimers. Trypsin, for example, is bound over a hundred times more tightly than lysozyme or hemoglobin, in spite of its lower pI.

Basic peptides are also strongly bound by 5a and **6a** (Table 4, last two rows). Even small Arg_4 almost reaches micromolar affinity in buffer towards the octamer.[41] This finding holds strong promise for immobilization of dendrimers on solid support for a potential development of new affinity chromatography material for Arg-tagged recombinant proteins. Preliminary experiments along these lines revealed

that a basic overexpressed protein can be enriched from its cell lysate by a single chromatography step over a sepharose resin carrying **5a**.

Conclusions

We have shown that single binding events, which are hard to detect in aqueous solution, can be gradually reinforced and multiplied into potent artificial hosts for biomacromolecules. If an increasing number of individual weak-binding sites for amino acid residues on protein surfaces are interconnected with flexible spacers, suitable complementary protein surfaces are ultimately bound in highly efficient 1:1 complexes, even in buffer with physiological salt concentrations ten thousand times higher. In our case, a weak lysine and arginine binder (K_a in pure water $<10\,M^{-1}$) was turned into a powerful receptor for basic proteins (K_D for **6a** and histone H1 <250 nM). Remarkably, even the octameric dendrimer forms strong complexes with small basic peptides. These new artificial protein receptors are therefore promising candidates for protein purification through Arg tags and potential molecular switches to turn protein function on and off.

Experimental Section

General Remarks

All reagents were purchased at the highest commercial grade and used as supplied. 3,5-bis(bromomethyl)benzaldehyde[1], benzene-1,3,5-tricarboxylic acid-tris[(2-ammonium-ethyl)amide]tristrifluoroacetate,[2] and 3,5-bis(dimethoxyphosphinylmethyl)benzoic acid[3] were prepared as described in the literature. All solvents were freshly distilled. The following anhydrous solvents were distilled from their drying agents: acetonitrile (calcium chloride), dichloromethane (calcium hydride), and methanol (magnesium).

Reactions were monitored by thin layer chromatography (TLC) with Merck silica-gel 60 F_{254} plates. Silica gel 60 for flash chromatography (230–400 mesh) was supplied by Merck. HPLC was performed on a Merck–Hitachi system with an L-7150 analytical pump, a K-1800 preparative pump, an L-7400 or K-2501 UV detector, and an L-7614 solvent degasser. Yields refer to chromatographically and spectroscopically pure compounds unless otherwise noted.

Melting points were determined on a Kofler Thermophan apparatus from Reichert and are uncorrected. ^{1}H and ^{13}C NMR spectra were recorded at 300 K on a Bruker Avance AMX 300, DRX 400, or DRX 500 spectrometer. ^{31}P NMR spectra were recorded on a Bruker Avance ARX 200 spectrometer. Chemical shifts are reported as δ values in ppm relative to tetramethylsilane as an internal standard; multiplicities are indicated by s (singlet), d (doublet), t (triplet), m (multiplet), and br (broad). ^{13}C NMR spectra are broadband decoupled and calibrated on the particular solvent signal. Low- and high-resolution electronic ionisation (EI) mass spectra were measured on a MAT 711 Finnigan spectrometer, low- and high-resolution electron spray ionisation (ESI) mass spectra were recorded on a MAT 95 S Finnigan spectrometer. Samples (20 μL) were introduced as 10^{-7} M solutions in HPLC-grade methanol at flow rates of 20 μL min^{-1}. Heated capillary temperature: 150 °C. Ion spray potential: 3.5 kV (positive ESI), 3.0 kV (negative ESI). About 20–30 scans were averaged to improve the signal-to-noise ratio.

UV/Vis experiments were performed on a U-3410 spectrophotometer from Hitachi in Helma cuvettes with 0.2 mm inner diameter.

Fluorescence experiments were performed on a Jasco FP-6500 spectrometer with a stirring unit and a Haake water-temperating unit.

Syntheses

3,5-Bis(diethoxyphosphinylmethyl)benzoic acid ethyl ester: A solution of 3,5-dimethylbenzoic acid (12.0 g, 80 mmol, 1.0 equiv) in tetrachloromethane (250 mL) with *N*-bromosuccinimide (30.0 g, 168 mmol, 1.1 equiv) and a catalytic amount of α,α′-azobisisobutyronitrile was heated at reflux for 4 h. The insoluble succinimide was filtered off, and the solvent was removed in vacuo. The remaining solid was dissolved in an excess of triethylphosphite (200 mL, 1.3 mol, ≈16 equiv), and the solution was heated at reflux for 5 h. The remaining solvent was removed in vacuo, and the resulting oil was purified by chromatography over silica with dichloromethane/methanol (19:1; $R_f=0.49$). Yield: 4.9 g (11 mmol, 14%). ^{1}H NMR (300 MHz, $CDCl_3$): $\delta=7.77$ (s, 2H), 7.35 (s, 1H), 7.53 (m, 1H), 4.26 (q, $^3J_{H,H}=7.0$ Hz, 2H), 3.89–3.99 (m, 8H), 3.08 (d, $^2J_{H,P}=21.9$ Hz, 4H), 1.29 (t, $^3J_{H,H}=7.0$ Hz, 3H), 1.16 ppm (t, $^3J_{H,H}=7.0$ Hz, 12H); ^{13}C NMR (75 MHz, $CDCl_3$): $\delta=165.9$, 135.3–135.5 (m), 132.3–132.4 (m), 130.8–130.9 (m), 129.2–127.4 (m), 60.9–62.1 (m), 60.9, 33.3 (d, $^1J_{C,P}=138.4$ Hz), 16.2–16.3 (m), 14.2 ppm; ^{31}P{^{1}H} NMR (81 MHz, $CDCl_3$): $\delta=26.5$ ppm (s).

3,5-Bis(diethoxyphosphinylmethyl)benzoic acid: 3,5-Bis(diethoxyphosphinylmethyl)benzoic acid ethyl ester (4.9 g, 10.8 mmol, 1 equiv) was dissolved in a mixture of methanol, tetrahydrofuran, and water (2:2:1 *v*/*v*/*v*), and the solution was cooled to 0 °C. Lithium hydroxide (520 mg, 21.5 mmol, 2 equiv) was added, and the solution was stirred for 7 h at 0 °C. The solvents were removed in vacuo, and the remaining solid was purified by chromatography over silica with dichloromethane/methanol (8:1; $R_f=0.28$). Yield: 1.0 g (2.4 mmol, 23%). M.p.: 109 °C; ^{1}H NMR (300 MHz, $CDCl_3$): $\delta=7.77$ (d, $^4J_{H,P}=2.0$ Hz, 2H), 7.40 (s, 1H), 3.94–4.09 (m, 8H) 3.18 (d, $^2J_{H,P}=22.0$ Hz, 4H), 1.23 ppm (t, $^3J_{H,H}=7.0$ Hz, 3H); ^{13}C NMR (75 MHz, $CDCl_3$): $\delta=168.1$, 135.2–135.4 (m), 132.0–132.1 (m), 131.6–131.7 (m), 130.1–130.2 (m), 62.6–62.7 (m), 33.4 (d, $^1J_{C,P}=138.4$ Hz), 16.3–16.4 ppm (m); ^{31}P{^{1}H} NMR (81 MHz, $CDCl_3$): $\delta=26.6$ ppm (s).

8-[3,5-Bis(dimethoxyphosphinylmethyl)benzoylamino]octyl-3,5-bis(dimethoxyphosphi-nylmethyl)benzamide: A solution of 3,5-bis(dimethoxyphosphonylmethyl)benzoic acid (250 mg, 0.68 mmol, 2.2 equiv) in anhydrous dichloromethane was treated with *N*-methyl-2-chloropyridiniumiodide (174 mg, 0.68 mmol, 2.2 equiv) and triethylamine (260 μL, 1.86 mmol, 6 equiv). The solution was stirred at ambient temperature for 10 min. 1,8-diaminooctane (45 mg, 0.31 mmol, 1 equiv) was then added, and the solution was stirred for 2 h. The solution was washed three times with acetic acid (1 N, 50 mL), saturated sodium hydrogencarbonate (50 mL), and water (50 mL). The organic phase was dried over magnesium sulfate and evaporated under reduced pressure. The crude product was purified by chromatography over silica with dichloromethane/methanol (19:1; $R_f=0.01$). Yield: 14 mg (0.17 mmol, 55%). ^{1}H NMR (200 MHz, $CDCl_3$): $\delta=7.59$ (s, 2H), 7.31 (s, 1H), 6.92 (t, $^3J_{H,H}=5.5$ Hz, 2H), 3.65 (d, $^3J_{H,P}=10.8$ Hz, 24H), 3.37 (m, 4H), 3.15 (d, $^2J_{H,P}=21.7$ Hz, 8H), 1.55–1.61 (m, 4H), 1.33 ppm (br, 8H); ^{13}C NMR (50 MHz, $CDCl_3$): 166.9, 135.8–135.9 (m), 133.4–133.7 (m), 131.8–132.1 (m), 127.1–127.3 (m), 52.8–53.0 (m), 40.0, 32.3, 29.3, 29.0, 26.8 ppm; ^{31}P{^{1}H} NMR (81 MHz, $CDCl_3$): $\delta=28.7$ ppm (s); HRMS (ESI) (pos., MeOH): *m*/*z* calcd: 840.2682 $[M+H]^+$; found: 841.275.

2: A solution of 8-[3,5-Bis(dimethoxyphosphinylmethyl)benzoylamino]octyl-3,5-bis(dimethoxyphosphinylmethyl)benzamide (70 mg, 83 μmol, 1 equiv) in anhydrous acetonitrile was heated at reflux with lithium bromide (32 mg, 0.37 μmol, 4.4 equiv) for 3 days. The resulting solid was filtered off and washed several times with acetonitrile. Yield: 54 mg (0.06 mmol, 80%). M.p.: >350 °C; ^{1}H NMR (200 MHz, D_2O): $\delta=7.39$ (s, 2H), 7.29 (s, 1H), 3.47 (d, $^3J_{H,P}=10.5$ Hz, 12H), 3.31 (t, $^3J_{H,H}=6.3$ Hz, 4H), 3.03 (d, $^2J_{H,P}=20.5$ Hz, 8H), 1.56 (br, 4H), 1.31 ppm (br, 8H); ^{13}C NMR (75 MHz, D_2O): $\delta=168.6$, 135.9–136.1 (m), 134.9–135.0 (m), 134.3–134.9 (m), 126.2–126.5 (m), 52.2–52.3 (m), 40.5, 33.8, 28.8, 26.6 ppm; ^{31}P{^{1}H} NMR (81 MHz, D_2O): $\delta=26.6$ ppm (s); HRMS (ESI) (pos., MeOH): *m*/*z* calcd: 803.1643 $[M+Na]^+$; found: 803.5320.

Benzene-1,3,5-tricarboxylic acid tris[3,5-bis(diethoxyphosphinylmethyl)-benzoylaminoethyl]amide: A solution of 3,5-bis(diethoxyphosphinylme-

thyl)benzoic acid (206 mg, 0.49 mmol, 3.3 equiv) in anhydrous acetonitrile (50 mL) was treated with *N*-methyl-2-chloropyridiniumiodide (136 mg, 0.53 mmol, 3.6 equiv) and triethylamine (300 μL, 2.21 mmol, 15 equiv). After 5 min, benzene-1,3,5-tricarboxylic acid tris[(2-ammoniumethyl)amide]tristrifluoroacetate[2] (100 mg, 0.15 mmol, 1.0 equiv) was added, and the mixture was stirred at ambient temperature for 24 h. After removal of the solvent in vacuo, the remaining crude product was purified over deactivated silica (activity level 5, 20% water) with ethyl acetate/methanol (2:1; $R_f = 0.11$). Yield: 110 mg (0.07 mmol, 48%). ^{1}H NMR (200 MHz, $CDCl_3$): $\delta = 8.43$–8.46 (m, 6H), 8.31 (s, 3H), 7.63 (d, $^4J_{H,P} = 2.0$ Hz, 6H), 7.22 (s, 3H), 3.84–3.99 (m, 24H), 3.52 (br, 12H), 3.09 (d, $^2J_{H,P} = 22.9$ Hz, 12H), 1.14 ppm (t, $^3J_{H,H} = 7.0$ Hz, 36H); ^{13}C NMR (75 MHz, $CDCl_3$): $\delta = 167.6$, 167.5, 134.9–135.0 (m), 134.5, 133.9–134.0 (m), 132.2–132.3 (m), 129.5, 127.5–127.7 (m), 62.6 (d, $^1J_{C,P} = 137.3$ Hz), 41.1, 40.1, 33.0, 16.1 ppm; ^{31}P{^{1}H} NMR (81 MHz, $CDCl_3$): $\delta = 26.4$ ppm (s). HRMS (ESI) (pos., MeOH): *m/z* calcd: 1571.5271 $[M+Na]^+$; found: 1571.3832.

3: A solution of benzene-1,3,5-tricarboxylic acid tris[3,5-bis(diethoxyphosphinylmethyl)benzoylaminoethyl]amide (110 mg, 71 μmol, 1.0 equiv) in anhydrous acetonitrile (15 mL) was treated with lithium bromide (41 mg, 469 μmol, 6.6 equiv) and heated at reflux for 7 days. The solid precipitated was filtered off and washed several times with acetonitrile. Yield: 60 mg (42 μmol, 60%). M.p.: 315°C; ^{1}H NMR (300 MHz, [D$_4$]MeOH): $\delta = 8.46$ (s, 3H), 7.56 (s, 6H), 7.36 (s, 3H), 3.74–3.83 (m, 12H), 3.61 (br, 12H), 2.95 (d, $^2J_{H,P} = 20.5$ Hz, 12H), 1.12 ppm (t, $^3J_{H,H} = 7.1$ Hz, 18H); ^{13}C NMR (75 MHz, [D$_4$]MeOH): $\delta = 171.4$, 169.0, 137.3–137.5 (m), 136.6–136.7 (m), 135.7–135.9 (m), 135.2, 130.3, 127.0–127.2 (m), 61.3-61.4 (m), 40.9, 40.7, 36.0 (d, $^1J_{C,P} = 129$ Hz), 17.1–17.2 ppm (m); ^{31}P{^{1}H} NMR (81 MHz, [D$_4$]MeOH): $\delta = 24.1$ (s); HRMS (ESI) (neg., MeOH): *m/z* calcd: 689.1602 $[M+4H^+]^{2-}$; found: 689.1570.

3,5-Bis(dimethoxyphosphinylmethyl)benzaldehyde: A solution of 3,5-bis(bromomethyl)benzaldehyde[1] (700 mg, 2.4 mmol) in an excess of pure trimethylphosphite (30 mL, 254 mmol) was heated at reflux for 4 h. The solvent was removed in vacuo, and the remaining yellowish oil was purified by chromatography on silica with dichloromethane/MeOH (20:1; $R_f = 0.32$). Yield: 770 mg (2.2 mmol, 92%). ^{1}H NMR (200 MHz, $CDCl_3$): $\delta = 9.99$ (s, 1H), 7.70 (m, 2H), 7.53 (m, 1H), 3.71 (d, $^3J_{P,H} = 11.0$ Hz, 12H), 3.23 ppm (d, $^2J_{P,H} = 22.0$ Hz, 4H); ^{13}C NMR (75 MHz, $CDCl_3$): $\delta = 191.6$, 136.9, 133.1, 131.9, 129.9, 129.6, 53.0 (d, $^1J_{P,C} = 6.7$ Hz), 32.3 ppm (d, $^2J_{P,C} = 138.2$ Hz); ^{31}P{^{1}H} NMR (81 MHz, $CDCl_3$): $\delta = 28.2$ ppm (s); elemental analysis: calcd (%) for $C_{13}H_{20}O_7P_2 \cdot 1.5\,H_2O$: C 41.39, H 6.14; found: C 41.55, H 5.96.

3,5-Bis[(methoxyphosphonyl)methyl]benzaldehyde dilithium salt: A solution of 3,5-bis(dimethoxyphosphinylmethyl)benzaldehyde (1.0 g, 2.9 mmol, 1.0 eq) and dried lithium bromide (0.5 g, 5.8 mmol, 2.0 equiv) in anhydrous acetonitrile (50 mL) was heated at reflux for 48 h under argon atmosphere. The precipitate was filtered off and washed several times with anhydrous acetonitrile. Yield: 870 mg (2.6 mmol, 90%). ^{1}H NMR (200 MHz, [D$_4$]MeOH): $\delta = 9.93$ (s, 1H), 7.71 (m, 2H), 7.58 (m, 1H), 3.51 (d, $^3J_{P,H} = 10.2$ Hz, 6H), 3.05 ppm (d, $^2J_{P,H} = 20.7$ Hz, 4H); ^{13}C NMR (75 MHz, D_2O): $\delta = 196.9$, 137.9 (t, $^3J_{P,C} = 5.6$ Hz), 136.5 (m), 129.3 (t, $^3J_{P,C} = 4.5$ Hz), 52.2 (d, $^1J_{P,C} = 6.2$ Hz), 33.6 ppm (d, $^2J_{P,C} = 128.1$ Hz); ^{31}P{^{1}H} NMR (81 MHz, [D$_4$]MeOH): $\delta = 25.2$ ppm (s); elemental analysis: calcd (%) for $C_{11}H_{14}Li_2O_7P_2 \cdot 1.5\,H_2O$: C 36.59, H 4.75; found: C 35.81, H 4.69.

General Procedure for the Synthesis of the Functionalized Dendrimers

A solution of 3,5-bis(methoxyphosphorylmethyl)benzaldehyde dilithium salt (100 mg, 0.3 mmol, 1.0 equiv in relation to the free ammonium groups of the PPI dendrimers) and the required PPI dendrimer (DAB-Am 4: 25 μL, 75.0 μmol, 0.25 equiv; DAB-Am 8: 26 mg, 37.5 μmol, 0.125 equiv; DAB-Am 16: 28 mg, 18.8 μmol, 0.063 equiv) (diaminobutane core dendrimer with 4, 8, and 16 amino groups, respectively) in anhydrous methanol (30 mL) were stirred under argon with molecular sieves (3 Å) at ambient temperature. After 72 h sodium borohydride (15 mg, 0,33 mmol, 1.1 equiv) was added, and the solution was stirred for another 24 h. The pulverized molecular sieves were filtered off, and the solvent was removed in vacuo. The remaining solid was purified by HPLC on a Nucleodur 00-5 CN-RP column with a gradient from 100% water (1% trifluoroacetic acid (TFA)) to 100% acetonitrile (1% TFA) and characterized as follows.

4: ^{1}H NMR (200 MHz, [D$_4$]MeOH): $\delta = 7.13$ (s, 12H), 3.81 (br s, 8H), 3.51 (d, $^3J_{P,H} = 10.5$ Hz, 24H), 3.00 (d, $^2J_{P,H} = 20.5$ Hz, 16H), 2.69 (br, 8H), 2.54 (br, 12H), 1.72 (br, 8H), 1.46 ppm (br, 4H); ^{31}P{^{1}H} NMR (81 MHz, [D$_4$]MeOH): $\delta = 27.47$ppm; MS (MALDI-TOF): *m/z*: 1541.7 $[M_{\text{protonated phosphonates}}+H]^+$.

5: ^{1}H NMR (300 MHz, [D$_4$]MeOH): $\delta = 7.16$ (m, 16H), 7.11 (s, 8H), 3.69 (s, 16H), 3.50 (d, $^3J_{P,H} = 10.2$ Hz, 48H), 2.96 (d, $^2J_{P,H} = 20.5$ Hz, 32H), 2.61 (br, 16H), 2.48 (br, 36H), 1.71 (br, 24H), 1.47 ppm (br, 4H); ^{31}P{^{1}H} NMR (81 MHz, [D$_4$]MeOH): $\delta = 26.24$ pm; MS (MALDI-TOF): *m/z*: 3321.7 $[M_{\text{Li salt}}+H]^+$.

6: ^{1}H NMR (300 MHz, [D$_4$]MeOH): $\delta = 7.13$ (m, 48H), 3.72 (br, 32H), 3.50 (d, $^3J_{P,H} = 10.2$ Hz, 96H), 3.00 (d, $^2J_{P,H} = 20.0$ Hz, 64H), 2.34–2.73 (br, 116H), 1.68 (br, 56H), 1.29 ppm (br, 4H); ^{31}P{^{1}H} NMR (81 MHz, [D$_4$]MeOH): $\delta = 25.83$; MS (MALDI-TOF): *m/z*: 3292.2 $[M_{\text{protonated phosphonates}}+2H]^{2+}$.

5a: A mixture of PPI dendrimer (DAB-Am 8: 50 mg, 64.7 μmol, 1.0 equiv) in 2 mL water and fluorescein, activated as *N*-hydroxysuccinimide ester (40 mg, 84.5 μmol, 1.3 equiv) in DMSO (400 μL), was incubated for 4 h. The solvent was removed, and 3,5-bis(methoxyphosphorylmethyl)benzaldehyde dilithium salt (160 mg, 447 μmol, 7.0 equiv) was added to the residue. The mixture was dissolved in anhydrous methanol (40 mL) and stirred under argon with molecular sieves (3 Å) at ambient temperature. After 24 h, sodium borohydride (20 mg, 0.440 mmol, 6.8 equiv) was added, and the solution was stirred for another 24 h. The pulverized molecular sieves were filtered off, and the solvent was removed in vacuo. The remaining solid was purified by dialysis with water for 4 days. Yield: 65 mg (19.3 μmol, 30%). ^{1}H NMR (300 MHz, D_2O): $\delta = 7.21$ (s, 21H), 4.14 (s, 12H), 3.54 (d, $^3J_{P,H} = 10.2$ Hz, 49H), 3.05 (d, $^2J_{P,H} = 20.4$ Hz, 48H), 2.83–2.88 (br, 14H), 2.56 (br, 42H), 1.65–1.86 (br, 42H), 1.52–1.60 ppm (br, 4H); ^{31}P{^{1}H} NMR (81 MHz, D_2O): $\delta =$ 23.60 ppm.

6a: A mixture of PPI dendrimer (DAB Am 16: 50 mg, 29.6 μmol, 1.0 equiv) in 2 mL water and fluorescein, activated as *N*-hydroxysuccinimide ester (14 mg, 29.1 μmol, 1.0 equiv) in DMSO (100 μL), was incubated for 4 h. The solvent was removed, and 3,5-bis(methoxyphosphorylmethyl)benzaldehyde dilithium salt (150 mg, 449 μmol, 15 equiv) was added to the residue. The mixture was dissolved in anhydrous methanol (40 mL) and stirred under argon with molecular sieves (3 Å) at ambient temperature. After 24 h, sodium borohydride (20 mg, 0.440 mmol, 15 equiv) was added, and the solution was stirred for another 24 h. The pulverized molecular sieves were filtered off, and the solvent was removed in vacuo. The remaining solid was purified by dialysis with water for 4 days. Yield: 38 mg (5.56 μmol, 18%). ^{1}H NMR (300 MHz, D_2O): $\delta = 7.20$ (m, 45H), 4.11 (br, 30H), 3.54 (d, $^3J_{P,H} = 7.4$ Hz, 96H), 3.03 (d, $^2J_{P,H} = 19.6$ Hz, 106H), 2.34–2.73 (br, 192H), 1.60–1.88 (br, 97H), 1.57 ppm (br, 4H); ^{31}P{^{1}H} NMR (81 MHz, [D$_4$]MeOH): $\delta = 23.98$, 23.45 ppm.

LED-PFG-DSTE Measurements of the Modified Dendrimers

pH dependence of diffusion constants: The measurements were performed on a Bruker Avance DRX 500 spectrometer in aqueous solution at 298 K with suppression of the water signal by saturation. The corresponding pulse program was the LED-PFG-DSTE (DSTE = double stimulated echo) sequence developed by Jerschow and Müller[34b] with a diffusion delay of 51 ms and a gradient length of 3 ms. Square shapes were used for the gradients created by the Bruker program DOSY, and the gradient strength was increased in 9 increments from 10% to 90% of $g_{max} = 53.5\ G\,cm^{-1}$. Diffusion coefficients were determined by linear regression fit in Origin to the Stejskal–Tanner plot.[5] Only the bisphosphonate-modified octamer was used for these measurements. The diffusion coefficients presented Table 1 are corrected according to the viscosity change followed with dioxane as internal standard.[6] The table shows the average of at least three measurements. The calculated hydrodynamic radii obtained through molecular-modeling calculations were compared with the radii calculated by the Stokes–Einstein equation [Eq. (1)]:[7,8]

$$r = \frac{k_B T}{6\pi\eta D_0} \quad (1)$$

Association constants determined by measurement of the diffusion constants: The measurements of the diffusion coefficients were similar to the pH-dependent measurements above. For constant pH, the measurements were performed in Na_2HPO_4/NaH_2PO_4 buffer (10 mM) at pH 7.1, and the coefficients were corrected by measuring dioxane as an internal viscosity standard. The binding constants were calculated according to Equation (2):[8]

$$K_d = P_0\left(\frac{D_b - D_0}{D_0 - D_f}\right) + L_0\left(\frac{D_0 - D_b}{D_b - D_f}\right) \quad (2)$$

where P_0 is the concentration of the protein, L_0 is the concentration of the dendrimer (each in the range 0.5–1.0 mM), D_b is the diffusion coefficient of the free protein, D_f is the diffusion coefficient of the free dendrimer, and D_0 is the average of the diffusion coefficients of the mixture. Analogous to the NMR spectroscopic titrations above, the concentrations of the host compound were multiplied to account for higher stoichiometries determined in the fluorescence titrations (Table 2).

UV/Vis Experiments

All functionalized dendrimers were titrated against Cyt *c*, and the absorbance at 409 nm (λ_{max} of the porphyrine ring) was observed. Cyt *c* was dissolved (50 nM) in phosphate-buffered water (10 mM, pH 7.1). The dendrimers were each dissolved in the solution of Cyt *c* to keep its concentration constant during the whole titration. It was checked that there was no measurable absorbance of the dendrimers at the observed wavelength. The change in the absorbance during the titration was taken as the basis for nonlinear regression methods to calculate the appropriate association constants. The related complex stoichiometries were determined by Job plots from the titration data and taken as the basis for the calculation of the binding constants.

Fluorescence Experiments

Fluorescence titrations with fluorescent-labeled proteins: The fluorescence titrations were performed in general with OregonGreen 488-labeled proteins, those with chymotrypsin also with fluorescein-labeled proteins. The active succinimidyl ester of OregonGreen 488 and the active *N*-hydroxysuccinimide ester of fluorescein were purchased from Molecular Probes and attached to the proteins according to the procedures provided by them (pH 8.4, water). The resulting compounds were purified by gel filtration on HiTrap™ desalting columns from Amersham Biosciences on an ÄKTA prime fast protein liquid chromatography (FPLC) system by Amersham Pharmacia Biotech with a flow rate of 1 mL min^{-1}. Na_2HPO_4/NaH_2PO_4 buffer (pH 7.1; 10 mM) containing NaCl (100 mM) was used as eluent. The protein solutions were concentrated and desalted by ultracentrifugation with Vivaspin MWCO PES filters from Vivascience/Sartorius.

The labeled proteins were used in phosphate-buffered solutions (10 mM, pH 7.1) in concentrations as stated in the Supporting Information. The dendrimers were diluted in the protein solutions, so that there was no change in the protein concentration during the titration. These solutions (400 or 700 μL) were placed in the cuvettes, and the dendrimer solutions (up to 300 μL) were added stepwise. The change in the emission intensity was traced (see Supporting Information). The same curve-fitting procedures as in the UV/Vis and NMR spectroscopic titrations were used to calculate the binding constants.

Fluorescence titrations with fluorescent-labeled dendrimers: These fluorescence titrations were performed with fluorescein-labeled **5a** and **6a**. Fluorescein, activated as the *N*-hydroxysuccinimide ester, was purchased from Molecular Probes and attached to the dendrimers as described in the synthesis section.

The labeled dendrimers were used in Hepes-buffered solutions (10 mM, pH 7.0) in concentrations as stated in the Supporting Information. In some cases, to reveal the effect of different buffers, the Hepes buffer was replaced by sodium phosphate buffer (10 mM, pH 7.1) or treated with sodium chloride (150 mM) (see Supporting Information).

Prior to the titrations, proteins were dissolved in dendrimer solutions of constant concentration, so that there was no change in the total dendrimer concentration during the titration. These solutions (400 μL) were placed in the cuvettes, and the protein solutions (100–700 μL) were added stepwise. The change in the emission intensity was traced (see Supporting Information). The same curve-fitting procedures as those used in the fluorescence titrations with labelled proteins were used to calculate the binding constants.

Acknowledgements

The authors are indebted to Dr. Uwe Linne for MALDI-TOF MS measurements. We thank Prof. Marahiel, Marburg, for the opportunity to perform GPC purifications in his group. We gratefully acknowledge generous support from Prof. Hynes, National University of Ireland, Galway, by providing his latest version of WinEQNMR.

[1] Review: M. Mammen, S. K. Choi, G. M. Whitesides, *Angew. Chem.* **1998**, *110*, 2908–2953; *Angew. Chem. Int. Ed.* **1998**, *37*, 2754–2794.
[2] For strongly enhanced polyvalent binding, a positive cooperativity in the classical sense is not required. For a rigorous definition of cooperativity (coupled binding steps) in biological systems, see: a) D. E. Koshland, K. Neet, *Annu. Rev. Biochem.* **1968**, *37*, 359–410; b) B. Perlmutter-Hayman, *Acc. Chem. Res.* **1986**, *19*, 90–96; cooperativity in self-assembly: c) G. Ercolani, *J. Am. Chem. Soc.* **2003**, *125*, 16097–16103.
[3] a) W. J. Lees, A. Spaltenstein, W. J. E. Kingery, G. M. Whitesides, *J. Med. Chem.* **1994**, *37*, 3419–3433; b) M. Mammen, G. Dahmann, G. M. Whitesides, *J. Med. Chem.* **1995**, *38*, 4179–4190.
[4] M. D. Pierschbacher, E. Ruoslathi, J. Sundelin, P. Lind, P. A. Peterson, *J. Biol. Chem.* **1982**, *257*, 9593–9595.
[5] a) A. Varki, *J. Clin. Invest.* **1997**, *99*, 158–162; b) J. B. Lowe, P. A. Ward, *J. Clin. Invest.* **1997**, *99*, 822–826.
[6] N. J. Dimmock, *Trends Biochem. Sci.* **1987**, *12*, 70–74.
[7] H. Chen, M. L. Privalsky, *Proc. Natl. Acad. Sci. USA* **1995**, *92*, 422–426.
[8] a) J. Rao, G. M. Whitesides, *J. Am. Chem. Soc.* **1997**, *119*, 10286–10290; b) J. Rao, J. Lahiri, L. Isaacs, R. M. Weis, G. M. Whitesides, *Science* **1998**, *280*, 708–711.
[9] P. I. Kitov, J. M. Sadowska, G. Mulvey, G. D. Armstrong, H. Ling, N. S. Pannu, R. J. Read, D. R. Bundle, *Nature* **2000**, *403*, 669–672.
[10] E. A. Merritt, Z. Zhang, J. C. Pickens, M. Ahn, W. G. J. Hol, E. Fan, *J. Am. Chem. Soc.* **2002**, *124*, 8818–8824.
[11] L. E. Strong, L. L. Kiessling, *J. Am. Chem. Soc.* **1999**, *121*, 6193–6196.
[12] a) A. Ojida, Y. Mito-oka, M. Inoue, I. Hamachi, *J. Am. Chem. Soc.* **2002**, *124*, 6256–6258; b) A. Ojida, M. Inoue, Y. Mito-oka, I. Hamachi, *J. Am. Chem. Soc.* **2003**, *125*, 10184–10185; c) A. Ojida, T. Kohira, I. Hamachi, *Chem. Lett.* **2004**, *33*, 1024–1025; review: d) A. Ojida, Y. Miyahara, T. Kohira, I. Hamachi, *Biopolymers* **2004**, *76*, 177–184.
[13] Md. A. Fazal, B. C. Roy, S. Sun, S. Mallik, K. R. Rodgers, *J. Am. Chem. Soc.* **2001**, *123*, 6283–6290.
[14] a) N. O. Fischer, C. M. McIntosh, J. M. Simard, V. M. Rotello, *Proc. Natl. Acad. Sci. USA* **2002**, *99*, 5018–5023; b) N. O. Fischer, A. Verma, C. M. Goodman, J. M. Simard, V. M. Rotello, *J. Am. Chem. Soc.* **2003**, *125*, 13387–13391.
[15] a) Q. Lin, H. S. Park, Y. Hamuro, C. S. Lee, A. D. Hamilton, *Biopolymers* **1998**, *47*, 285–297; b) H. S. Park, Q. Lin, A. D. Hamilton, *J. Am. Chem. Soc.* **1999**, *121*, 8–13; c) R. K. Jain, A. D. Hamilton, *Org. Lett.* **2000**, *2*, 1721–1723; d) L. Baldini, A. J. Wilson, J. Hong, A. D. Hamilton, *J. Am. Chem. Soc.* **2004**, *126*, 5656–5657.

[16] a) R. Fasan, R. L. A. Dias, K. Moehle, O. Zerbe, J. W. Vrijbloed, D. Obrecht, J. A. Robinson, *Angew. Chem.* **2004**, *116*, 2161–2164; *Angew. Chem. Int. Ed.* **2004**, *43*, 2109–2112; b) Z. Athanassiou, R. L. A. Dias, K. Moehle, N. Dobson, G. Varani, J A. Robinson, *J. Am. Chem. Soc.* **2004**, *126*, 6906–6913.
[17] a) K. Enander, G. T. Dolphin, L. Baltzer, *J. Am. Chem. Soc.* **2004**, *126*, 4464–4465; b) P. Rossi, P. Tecilla, L. Baltzer, P. Scrimin, *Chem. Eur. J.* **2004**, *10*, 4163–4170.
[18] a) T. Schrader, *Chem. Eur. J.* **1997**, *3*, 1537; b) T. Schrader, M. Wehner, P. Finocchiaro, S. Failla, G. Consiglio, *Org. Lett.* **2000**, *2*, 605–608; c) S. Rensing, A. Springer, T. Grawe, and T. Schrader, *J. Org. Chem.* **2001**, *66*, 5814–5821; d) S. Rensing, T. Schrader, *Org. Lett.* **2002**, *4*, 2161–2164.
[19] a) H. J. Schneider, R. Kramer, S. Simova, U. Schneider, *J. Am. Chem. Soc.* **1988**, *110*, 6442; b) C. S. Wilcox in *Frontiers in Supramolecular Chemistry* (Ed.: H. J. Schneider), Verlag Chemie, Weinheim, **1991**, p. 123.
[20] a) S.-E. Stiriba, H. Frey, R. Haag, *Angew. Chem.* **2002**, *114*, 1385–1390; *Angew. Chem. Int. Ed.* **2002**, *41*, 1329–1334; b) R. Haag, *Angew. Chem.* **2004**, *116*, 280–284; *Angew. Chem. Int. Ed.* **2004**, *43*, 278–282.
[21] Similar conclusions have already been postulated from scanning force microscopy (SFM) measurements on nonnatural surfaces: a) I. Gössl, L. Shu, A. D. Schlüter, J. P. Rabe, *J. Am. Chem. Soc.* **2002**, *124*, 6860–6865; for structural, morphological, and pharmaceutical properties of dendrimers, see: b) A. W. Bosman, H. M. Janssen, E. W. Meijer, *Chem. Rev.* **1999**, *99*, 1665–1688; c) M. Liu, J. M. Frechet, *Pharm. Sci. Technol. Today* **1999**, *2*, 393–401.
[22] B. L. Nilsson, L. L. Kiessling, R. T. Raines, *Org. Lett.* **2001**, *3*, 9–12.
[23] L. Eckardt, K. Naumann, W. M. Pankau, M. Rein, M. Schweitzer, N. Windhab, G. von Kiedrowski, *Nature* **2002**, *420*, 286.
[24] Review: a) H. C. Kolb, M. G. Finn, K. B. Sharpless, *Angew. Chem.* **2001**, *113*, 2056–2075; *Angew. Chem. Int. Ed.* **2001**, *40*, 2004–2021; b) R. Manetsch, A. Krasinski, Z. Radic, J. Raushel, P. Taylor, K. B. Sharpless, H. C. Kolb, *J. Am. Chem. Soc.* **2004**, *126*, 12809–12818; c) N. J. Agard, J. A. Prescher, C. R. Bertozzi, *J. Am. Chem. Soc.* **2004**, *126*, 15046–15047.
[25] Recently, DNA-catalyzed polymerization was performed with a stepwise reductive amination of a thymidine aminoaldehyde monomer: X. Li, Z.-Y. J. Zhan, R. Knipe, D. G. Lynn, *J. Am. Chem. Soc.* **2002**, *124*, 746–747.
[26] a) R. Karaman, A. Goldblum, E. Breuer, *J. Chem. Soc. Perkin Trans. 1* **1989**, 765–774; b) H. Krawczyk, *Synth. Commun.* **1997**, *27*, 3151–3161.
[27] Contrary to most procedures, $NaBH_3CN$ turned out to be completely unreactive towards the imine intermediate and was therefore replaced by $NaBH_4$.
[28] Typically, the imine resonance at 8.1 ppm was completely converted into a benzylamine signal at 3.7 ppm (Figure 3).
[29] For details and a typical MALDI spectrum, see Supporting Information.
[30] C. S. Johnson, *Prog. Nucl. Magn. Reson. Spectrosc.* **1999**, *34*, 203–256.
[31] MacroModel 7.0, Amber* force field, water, 2000 steps.
[32] a) I. Lee, B. D. Athey, A. W. Wetzel, W. Meixner, J. R. Baker, *Macromolecules* **2002**, *35*, 4510; b) W. Chen, D. A. Tomalia, J. L. Thomas, *Macromolecules* **2000**, *33*, 9169.
[33] a) D. A. Tomalia, A. M. Naylor, W. A: Goddard, *Angew. Chem.* **1990**, *102*, 119–157; *Angew. Chem. Int. Ed. Engl.* **1990**, *29*, 138–175; b) Y. Kim, C. Zimmerman, *Curr. Opin. Chem. Biol.* **1998**, *2*, 733–742.
[34] a) I. B. Rietveld, D. Bedeaux, *Macromolecules* **2000**, *33*, 7912; b) A. Jerschow, N. Muller, *J. Magn. Reson.* **1997**, *125*, 372–75.
[35] a) D. K. Wilkins, S. B. Grimshaw, V. Receveur, C. M. Dobson, J. A. Jones, L. J. Smith, *Biochemistry* **1999**, *38*, 16424; b) A. M. Weljie, A. P. Yamniuk, H. Yoshino, Y. Izumi, H. J. Vogel, *Protein Sci.* **2003**, *12*, 228; c) L. H. Lucas, C. K. Larive, *Concepts Magn. Reson. Part A* **2004**, *20*, 24.
[36] The respective stoichiometries were determined from the subsequent UV/Vis and fluorescence titrations.
[37] K. A. Connors, *Binding Constants*, Wiley, New York, **1987**.
[38] Molecular Probes, http://www.molecularprobes.com/media/pis/mp06153.pdf.
[39] It should be noted, however, that peptide titrations did not confirm general lysine selectivity (Table 2).
[40] M. J. Hynes, *J. Chem. Soc. Dalton Trans.* **1993**, 311–312.
[41] Unfortunately, Arg_6 affinity drops drastically if Hepes buffer is replaced by phosphate buffer (pH 7.0).

Received: April 21, 2006

